A multiple-reach model describing the migratory behavior of Snake River yearling chinook salmon (*Oncorhynchus tshawytscha*)

Richard W. Zabel, James J. Anderson, and Pamela A. Shaw

Abstract: A multiple-reach model was developed to describe the downstream migration of juvenile salmonids in the Columbia River system. Migration rate for cohorts of fish was allowed to vary by reach and time step. A nested sequence of linear and nonlinear models related the variation in migration rates to river flow, date in season, and experience in the river. By comparing predicted with observed travel times at multiple observation sites along the migration route, the relative performance of the migration rate models was assessed. The analysis was applied to cohorts of yearling chinook salmon (*Oncorhynchus tshawytscha*) captured at the Snake River Trap near Lewiston, Idaho, and fitted with passive integrated transponder (PIT) tags over the 8-year period 1989–1996. The fish were observed at Lower Granite and Little Goose dams on the Snake River and McNary Dam on the Columbia River covering a migration distance of 277 km. The data supported a model containing two behavioral components: a flow term related to season where fish spend more time in regions of higher river velocity later in the season and a flow-independent experience effect where the fish migrate faster the longer they have been in the river.

Résumé : Un modèle sur tronçons multiples a été élaboré pour décrire la dévalaison de salmonidés juvéniles dans le réseau du Columbia. Le taux de migration des cohortes de poissons pouvait varier en fonction du tronçon et de l'intervalle de temps. Une séquence hiérarchique de modèles linéaires et non linéaires liait la variation du taux de migration au débit de la rivière, au moment de la saison, et à la connaissance de la rivière. En comparant les temps de déplacement prévus et les temps observés à plusieurs points d'observation situés le long de la route migratoire, on a évalué la performance relative des modèles des taux de migration. L'analyse a été appliquée à des cohortes de saumons quinnats (*Oncorhynchus tshawytscha*) âgés de 1 an, capturés dans la trappe située sur la Snake près de Lewiston (Idaho) et auxquels on avait fixé des marques PIT (à transpondeur intégré passif), pendant une période de 8 ans (1989–1996). Les poissons ont été observés aux barrages de Lower Granite et de Little Goose sur la Snake et au barrage McNary sur le Columbia, ce qui couvre une distance de migration de 277 km. Les données appuient un modèle renfermant deux composantes du comportement : un effet de débit lié à la saison pour lequel les poissons restent plus longtemps dans les régions où la vitesse de la rivière est élevée tard dans la saison et un effet de connaissance de la rivière, indépendant du débit, pour lequel plus le temps de séjour du poisson dans la rivière est long, plus sa migration est rapide.
[Traduit par la Rédaction]

Introduction

The behavior of juvenile salmon during their migration from tributary streams to the ocean is highly variable (Groot and Margolis 1991) and depends on a variety of factors. These factors may be inherent to the fish's condition such as size (Washington 1982) and level of smoltification (Hoar 1976; Folmar and Dickhoff 1980), and they may be external factors such as river flow (Berggren and Filardo 1993) and river temperature (Brett et al. 1958). The knowledge of migration behavior and the ability to predict migration speed have practical value in rivers with hydroelectric systems. Such information can be used to partially mitigate the impacts of hydroelectric dams on the fish and thus improve migration survival.

For some stocks of juvenile salmon, travel times through the Snake and Columbia rivers have doubled as the result of river impoundment by dams (Raymond 1979), and thus, mitigation efforts have focused on improving fish migration speed under the assumption that faster migration may improve fish survival. In the Snake River Salmon Recovery Plan for the Endangered Species Act (NMFS 1995), it was assumed that fish speed could be increased by increasing water velocity. Two strategies were proposed to increase water velocity: (*i*) augmenting flow with water from storage reservoirs in the upper Columbia and Snake rivers or (*ii*) lowering reservoir levels behind the dams (drawdown) on the mainstem Columbia and Snake rivers. Both actions have ecological and economic consequences. Draining the upriver storage reservoirs for the spring migration adversely affects resident fish in the storage reservoirs and uses water that could otherwise be used for power generation, irrigation, or flow augmentation for summer migrants. Drawdown has a number of unknown ecological impacts on the riverine habitat and complicates the dam passage of both juvenile and adult salmon. Thus, whichever method is used to increase water velocity, it is essential to implement the action in the most effective manner possible to increase fish velocity.

This paper presents a mathematical model for fish migration

Received October 15, 1996. Accepted June 24, 1997.
J13702

R.W. Zabel,[1] J.J. Anderson, and P.A. Shaw. University of Washington, Box 358218, Seattle, WA 98195-8218, U.S.A.

[1] Author to whom all correspondence should be addressed.
e-mail: rich@cqs.washington.edu

behavior that captures many of the basic factors controlling juvenile salmonid migration rate. It builds on earlier work that modeled the downstream movement of a cohort of fish through a single river reach, a reach being defined as a stretch of river delineated by a dam or a major confluence. The model was defined by two parameters: a mean migration rate and a rate of population spreading (Zabel and Anderson 1997). We extend the model to multiple reaches and identify environment- and fish-specific factors that relate juvenile spring chinook salmon (*Oncorhynchus tshawytscha*) migration rate. In addition, we develop statistical methods to extract parameters from arrival time data of fish observed at several points along the migration route. This allows for the determination of a change in migration rate as the fish progress down the river.

Using a nested sequence of nonlinear models, we related migration rate of Snake River yearling chinook to river flow, date in the season, and length of time in the river to determine the importance of these factors as formulated in the models. Also, to demonstrate the utility of the model as a predictive tool, we generated predictions of 1996 arrival distributions based on independent data and then compared the predictions with the observations.

Methods

Multiple-reach model

To develop the multiple-reach model, we begin with a description of the single-reach model. In this model, a point release of fish migrates through a reach based on an advection–diffusion equation with an absorbing boundary at the end of the reach (Zabel 1994; Zabel and Anderson 1997). The resulting travel time distribution, sometimes called the inverse Gaussian distribution, is based on reach length (L) and two parameters: downstream migration rate, r, and the rate of population spreading, σ^2.

The travel time distribution can be described in terms of

(1) p_t = Prob(arriving during tth time period, given values r, σ^2, and L)

with $t = (1, 2, 3,...)$. If there are N recaptured individuals in the cohort, then

(2) $\hat{n}_t = N \cdot p_t$ = expected number of individuals arriving during tth time period.

The travel time distribution has a long right tail (Fig. 1) and fits well to observed travel time distributions (Zabel and Anderson 1997).

The single-reach model is connected in a serial sequence to move a cohort of fish through multiple reaches. All the fish in the cohort are assumed to have identical statistical characteristics but are assumed to be independent. The model begins with a point release at the head of the uppermost reach. This cohort's arrival time distribution at the end of the first reach is based on the single-reach model. This arrival distribution is then used as a departure distribution for the next reach. The model iterates through each departure time and distributes these fish at the next downstream site. Fish departing during different time intervals from an upstream site but arriving at a downstream site in the same time interval are combined in the arrival time distribution. The new arrival time distribution is then used as a departure distribution for the next reach. This cohort of fish is moved from reach to reach in this manner until the fish arrive at the end of the river.

The number of fish arriving at the ith site during the tth time step, $n_{i,t}$, is calculated as

$$(3) \qquad n_{i,t} = \sum_{j=1}^{t-1} n_{i-1,j} \cdot P_{t-j} \cdot S_{i,t-j} \cdot (1 - T_{i-1,j})$$

Fig. 1. Travel time distribution from the single-reach model. For this plot, $r = 5$ km·day^{-1}, $\sigma^2 = 100$ km^2·day^{-1}, reach length = 50 km, and population size = 100 fish.

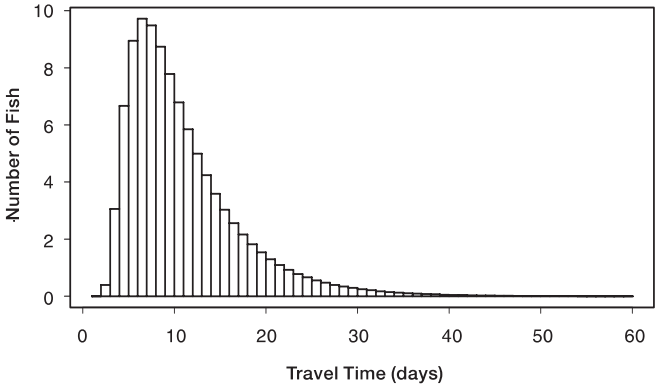

where $S_{i,t-j}$ is the probability of surviving from the $(i-1)$th to the ith site during the $(t-j)$ time steps and $T_{i-1,j}$ is the probability of being transported out of the system from the $(i-1)$th site during the jth time step. The first two terms inside the summation multiply the probability of a fish departing from the upstream site during the jth time period by the probability of the fish taking exactly $t-j$ time steps to travel through the reach. The summation is over all the combinations of departure times and travel times that result in fish arriving at the ith site during the tth time step. The last two terms adjust the numbers for survival and collection of fish for transportation through the river in barges, respectively. Since these processes are time dependent, they can affect the shape of the predicted arrival time distributions and will be described in more detail below.

The mean travel time to the ith site is computed as

$$(4) \qquad \hat{\bar{T}}_i = \frac{1}{N_i} \sum_{t=1}^{S} t \cdot n_{i,t}$$

where S is the length of the migratory season and N_i is the total number of fish observed at the ith site. These expected mean travel times were compared with the observed ones in the statistical analysis.

Migration rate equations

To implement the model, migration rates, r_t (in kilometres per day), on a per reach and per time step basis are expressed through flow-related and flow-independent terms. Both terms are time dependent, reflecting the change in fish behavior through time. Any number of mathematical equations can be used to express how the two migration components evolve over time. We formulated a sequence of models below to explore the mechanisms that determine change in migration rate with conditions.

Migration rate model 1: The null model assumes that r is described by a mean rate β_0:

$$(5) \qquad r_t = \beta_0 + \varepsilon_t.$$

Variation about the mean rate is expressed by ε_t.

Migration rate model 2: This model assumes a linear relationship between migration rate and river velocity:

$$(6) \qquad r_t = \beta_0 + \beta_1 \bar{V}_t + \varepsilon_t$$

where $\bar{V}_t$ is the mean velocity during the mean migration period for each of the reaches. River velocity is calculated from river flow, F_t, through a dimensional equation:

$$(7) \qquad V_t = \frac{F_t}{X}$$

where X is the cross-sectional area of the reservoir. The intercept (β_0) is a combination of directed movement independent of flow and a potential nonzero intercept from the river velocity/river flow relationship.

Migration rate model 3: This model assumes that fish migrate more actively later in the season by migrating in the higher flow regions of the river and (or) by spending a greater proportion of the day in the river flow versus holding up along the shore. This is achieved by weighting river velocity with a term that increases as t increases. The equation is formulated as

$$(8) \qquad r_t = \beta_0 + \beta_{FLOW}\overline{V}_t\left[\frac{1}{1+\exp(-\alpha_2(t-T_{SEASN}))}\right] + \varepsilon_t$$

where t is the day of the year in the migratory season. Equation 8 is based on the following four parameters: β_0, determines the flow-independent migration (kilometres per day); β_{FLOW}, determines the proportion of the river velocity used for downstream migration when the fish are fully smolted (nondimensional); α_2, slope parameter that determines how quickly the flow effects shift from early-season to late-season behavior (per day); T_{SEASN}, inflection point of the flow-dependent term that has the effect of shifting the flow effect through the season (day of the year); previous to this date, fish use less flow for migration, and after it, they use more.

Migration rate model 4: The model has the same terms as model 3 plus a flow-independent experience factor: as fish spend more time in the river, migration speed is increased. Migration rate for the ith release group is modeled as

$$(9) \qquad r_t = \beta_0 + \beta_1\left[\frac{1}{1+\exp(-\alpha_1(t-T_{RLS}))}\right] + \beta_{FLOW}\overline{V}_t\left[\frac{1}{1+\exp(-\alpha_2(t-T_{SEASN}))}\right]$$

Equation 9 introduces the following terms: T_{RLS}, release date (day of the year) for the cohort; α_1, slope parameter that determines rate of change of the experience effect (per day); β_0 and β_1, determine the magnitude of the flow-independent migration rate (kilometres per day). β_0 and β_1 are combined in the following way to determine the flow-independent contribution to migration rate:

$\beta_{MIN} = \beta_0 + \beta_1/2$ (minimum flow-independent migration rate at $t = T_{RLS}$)

$\beta_{MAX} = \beta_0 + \beta_1$ (maximum flow-independent migration rate as t gets large).

Both models 3 and 4 use the nonlinear logistic equation in which upper and lower bounds for migration rate can be set. This appears to be consistent with some types of juvenile salmon migratory behavior and eliminates unrealistically high or low migration rates that can occur with linear equations applied outside the range of observations. The flow-related term determines the seasonally varying proportion of river velocity used by fish for migration, and the inflection point, T_{SEASN}, shifts the effect of this term in the season. The flow-independent term is based on the fish's contribution to downstream migration, which increases with time spent in the river. For this term, the inflection point, T_{RLS}, is the release date for each cohort. This results in the desired functional form of a flow-independent contribution of β_{MIN} when the fish are released and β_{MAX} as t gets large.

Model implementation

The models were run utilizing the Columbia River Salmon Passage (CRiSP) model, a management tool for evaluating the effect of Columbia River hydrosystem operations on juvenile salmon (Anderson et al. 1996). The CRiSP model implements the migration rate models described above. In addition, it estimates the survival term in eq. 3. Mortality is imposed at the dams and in the reservoirs due to predation and gas bubble disease. The modeled survival was calibrated to survival studies (Iwamoto et al. 1994; Muir et al. 1995, 1996) based on fish of similar origin migrating through the same reaches as the ones we analyze below. In addition, the model keeps track of the numbers of fish collected at dams and barged through the system for release below the last dam on the river. As stated above, the number of fish transported and survival rates vary throughout the season and thus affect the shape of the arrival distributions. This information is needed to accurately predict mean travel times.

Statistical methods

The objectives of the statistical analysis were to estimate parameters and standard errors, assess how well the models compare with the data, and determine the appropriate level of complexity for the migration rate models.

Estimating parameters

The modeled mean travel times are a function of the model chosen and the particular parameter values selected. The migration rate parameters were estimated by a least-squares minimization (with respect to the parameters) of the following equation:

$$(10) \qquad SS = \sum_{i=1}^{O}\sum_{k=1}^{C}(\hat{\overline{T}}_{i,k} - \overline{T}_{i,k})^2$$

where O is the total number of observation sites, C is the total number of cohorts, $\hat{\overline{T}}_{i,k}$ is the modeled mean travel time to the ith site by the kth cohort, and $\overline{T}_{i,k}$ is the observed mean travel time to the ith site by the kth cohort. This equation was fit using a Levenberg–Marquardt routine (Fletcher 1990; Press et al. 1994), with derivatives calculated numerically using a finite-difference method (Gill et al. 1981; Seber and Wild 1989).

Standard errors

Approximate standard errors of the parameters were calculated following procedures for nonlinear least-squares regression (Bates and Watts 1988). The model function was linearized at the optimal parameter values, and then, linear least-squares calculations were implemented (Weisberg 1980). Since these values are approximate, they were not used for inference but rather to characterize the stability of the parameter estimates.

Estimating rate of population spreading

To implement the reach model, the rate of spreading (σ^2) of the cohorts must also be specified. The units for σ^2 are kilometres-squared per day. Although σ^2 is also variable from cohort to cohort (Zabel and Anderson 1997), the travel time model predictions are not as sensitive to variability in σ^2 as to variability in migration rate (Zabel 1994). For this paper, we treat it as constant among all cohorts to simplify the analysis.

The estimate of σ^2 is based on the spread of the travel time distribution; this information is lost when computing mean travel times. Thus, σ^2 is estimated separately after the migration rate parameters are estimated using eq. 10. To estimate σ^2, a finer resolution of the data is used. The unit of comparison between the model and the data is the number of individuals from each cohort observed per time step at each of the observation sites. Since the variance associated with this measure is highly variable, generalized least squares (Draper and Smith 1981; Seber and Wild 1989) was used, where each element of the summation is weighted by the variance. The equation to be minimized is

$$(11) \qquad SS = \sum_{i=1}^{O}\sum_{j=1}^{C}\sum_{t=1}^{S}\frac{1}{V_{ijt}}(n_{ijt} - \hat{n}_{ijt})^2$$

Fig. 2. Map of the migratory route along the Snake and Columbia rivers in Washington, Oregon, and Idaho (state boundaries shown by broken lines). The bars represent dams. Included are the release point (grey circle) and observation points (labeled dams). The river flow, in general, is from east to west. The area of detail is delineated by the rectangle in the inset map of the northwestern United States.

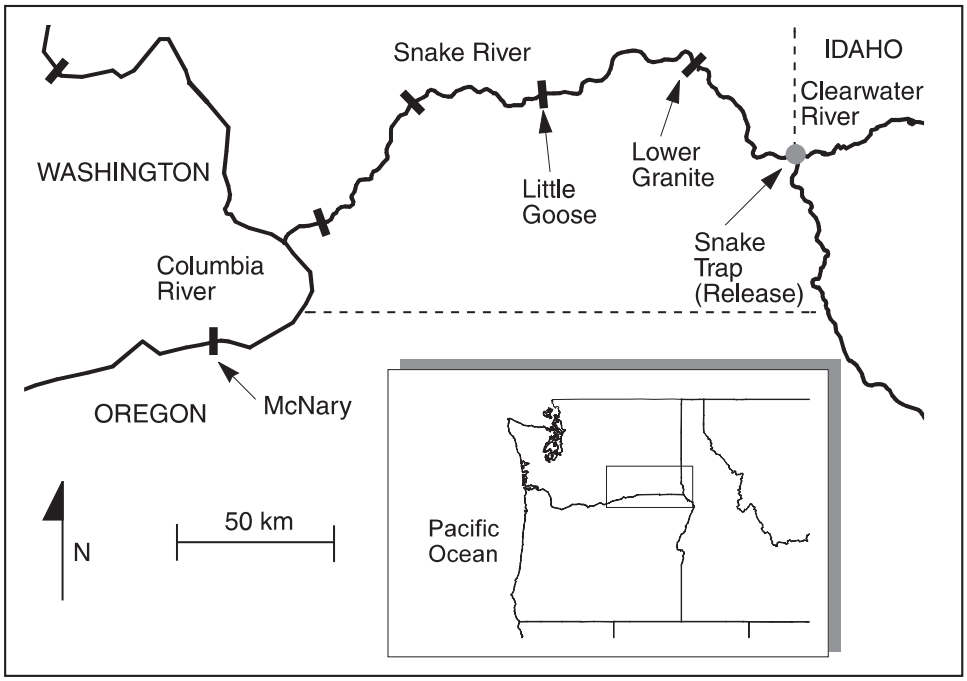

where n_{ijt} is the observed number of fish arriving at the ith site from the jth cohort during the tth time period and $\hat{n}_{ijt}$ is the expected number. V_{ijt} is the variance (under a multinomial model, see Zabel 1994) associated with this group and is calculated as

$$V_{ijt} = n_{ij} \cdot \hat{p}_{ijt} \cdot (1 - \hat{p}_{ijt}) \quad (12)$$

where n_{ij} is the number of fish from the jth cohort observed at the ith site. Equation 11 was also fit using a Levenberg–Marquardt routine, and the standard error was calculated in the same manner as with the migration rate parameters.

Model comparisons

To compare the performance of the migration models, a modified R^2 value is reported as the sum of squares of each model as compared with the sum of squares of the mean model (model 1):

$$R^2 = \frac{SS_1 - SS_A}{SS_1} \quad (13)$$

where SS_1 is the sum of squares for the mean model and SS_A is the sum of squares for the more complex (alternative) model. The R^2 value gives the percent reduction in the sum of squares for the alternative model as compared with the null model.

Standard statistical analysis of the results was not possible. In most cases, the residuals were not normally distributed, serial trends existed, and mean travel times were not independent from site to site within cohorts, making traditional F-tests invalid. However, many conclusions could be drawn about the models' performances based on the R^2 values and the standard errors of the parameter estimates.

Data

Passive integrated transponder (PIT) tags were used to monitor individual fish. The 12-mm tag, containing a microchip programmed with individual fish identification codes, was inserted in the fish's body cavity (Prentice et al. 1990). The system records passage times of individuals at interrogation sites. The tags do not seem to adversely affect the fish in terms of survival or swimming performance (Prentice et al. 1990).

The model was evaluated with "run-of-the-river" fish (hatchery and wild stocks) yearling chinook. The fish were captured, tagged, and released at the Snake River Trap by the Idaho Department of Fish and Game (Buettner and Nelson 1990) and observed at Lower Granite, Little Goose, and McNary dams over a migratory route of 277 km (Fig. 2). We analyzed daily releases from April 1 to May 12. Although these fish were classified as run-of-the-river, it is likely that the majority were yearling chinook based on the length distributions (most fish >110 mm) and the timing of migration (early spring). We did not analyze fish released after May 12, as length distributions indicated a possible presence of subyearling chinook which have different migratory behavior.

Release cohorts were formed by combining releases from up to 3 consecutive days to achieve sample sizes of at least 80 individuals observed at Lower Granite Dam. Seventy-eight cohorts were analyzed representing releases from 1989 to 1996. Table 1 contains release dates, mean travel times to the three observation sites, and sample sizes for all the cohorts. Water flow and reservoir geometry information was obtained from the Army Corps of Engineers.

The data yielded information on mean travel times from the release site to each of the three observation sites. Previous to 1993, most of the fish observed at a site were subsequently transported out of the hydrosystem. Thus, fish observations at more than one site were rare, resulting in limited intersite travel time information. We chose to include the first 4 years of data (and thus eliminate the possibility of interdam travel time analysis) to increase sample size and include a wider variety of river conditions; 1992, in particular, was an extremely low-flow year.

Predictions

Using river flow information and parameters estimated from the 1989–1995 data, we predicted cumulative passage distributions for the 1996 fish at the three downstream observation sites. These predictions were derived from the parameters estimated from the

Table 1. Mean release date, mean and standard deviation of travel times (TT, days), and number of fish observed from Snake River Trap to each observation site for each cohort.

Mean release date (day of the year)	Observation site								
	Lower Granite Dam			Little Goose Dam			McNary Dam		
	Mean	SD	*N*	Mean	SD	*N*	Mean	SD	*N*
1989									
94.9	15.7	6.9	97	21.0	5.9	77	28.8	6.2	46
97.4	14.4	6.8	110	19.7	5.7	128	27.2	7.0	71
99.8	16.1	9.0	97	20.4	7.7	78	27.6	7.3	46
101.9	11.8	5.6	103	17.7	7.0	85	23.0	8.9	37
104.0	9.5	4.5	119	16.0	6.3	68	24.4	6.8	44
105.9	8.5	5.1	119	13.6	6.4	73	20.5	8.3	40
108.0	6.7	5.0	130	11.4	4.7	75	17.4	4.7	36
109.9	5.9	3.8	122	12.1	4.8	78	19.9	7.5	33
111.9	6.2	3.5	122	12.4	4.2	53	17.5	5.4	35
113.9	7.1	4.6	130	12.7	4.3	67	18.9	5.6	39
115.9	7.3	3.2	136	11.7	4.5	52	17.4	4.7	32
117.8	7.1	3.9	103	11.8	4.1	38	16.2	3.2	19
1990									
107.3	6.3	3.0	80	16.4	8.7	39	18.8	4.2	12
109.0	6.1	2.8	93	14.9	6.4	41	20.4	6.2	32
110.9	8.2	6.5	118	15.4	6.5	44	21.6	6.9	38
112.9	8.9	5.5	128	16.9	8.3	46	20.8	5.2	30
114.7	11.2	7.5	106	15.9	5.8	32	22.1	4.6	22
1991									
98.9	16.9	6.5	97	23.8	5.3	51	33.7	7.1	20
100.6	15.4	5.8	89	20.0	3.5	33	28.2	6.3	15
102.5	14.4	5.4	94	19.6	5.2	34	27.2	4.2	14
106.4	14.8	6.8	143	19.6	6.3	60	26.0	5.6	30
108.9	13.2	5.3	102	17.3	5.1	52	22.4	4.1	16
112.9	10.4	5.4	127	16.1	7.7	55	22.0	5.6	19
116.4	7.8	4.9	90	12.4	4.8	33	18.2	3.5	27
115.9	9.0	4.5	84	16.3	4.9	31	18.4	2.8	15
117.6	9.5	4.2	101	14.1	4.1	34	20.2	6.8	10
119.9	8.9	3.9	99	13.8	4.5	30	20.1	3.4	15
1992									
99.2	13.6	6.7	107	19.3	6.7	53	28.8	5.7	33
105.3	12.8	6.4	115	16.9	4.7	49	23.6	6.4	25
1993									
100.0	14.0	5.1	118	20.4	3.7	90	27.9	2.9	45
101.8	14.8	5.1	119	20.4	4.1	95	26.6	3.3	48
110.7	9.7	3.5	92	13.3	3.1	59	19.5	3.4	21
112.9	8.0	3.1	82	13.0	3.8	40	17.3	3.3	23
114.9	7.0	2.3	94	9.8	2.0	62	16.2	2.5	40
117.0	6.3	2.3	115	10.3	2.9	58	15.5	2.9	28
119.0	5.7	2.6	101	10.3	3.0	43	14.3	2.5	30
121.0	4.9	1.9	113	9.1	2.3	60	13.2	1.9	25
122.9	4.2	1.5	113	8.1	2.0	65	12.5	2.9	29
124.6	4.0	2.1	98	9.2	3.0	27	12.5	2.3	8
125.9	4.8	2.1	141	9.3	2.8	51	14.1	3.7	30
127.6	5.6	2.6	107	9.7	3.4	27	13.9	4.7	21
130.0	5.4	2.0	96	9.0	2.7	39	12.6	2.4	29
132.0	4.3	2.3	84	8.6	6.4	30	12.9	7.1	32
1994									
104.2	10.8	4.3	80	16.3	5.3	67	26.4	5.7	70
109.9	7.6	4.1	92	14.3	6.6	28	23.3	5.7	47
111.0	7.7	4.3	149	13.0	5.4	68	23.8	5.9	106

Table 1 (*concluded*).

Mean release date (day of the year)	Observation site								
	Lower Granite Dam			Little Goose Dam			McNary Dam		
	Mean	SD	*N*	Mean	SD	*N*	Mean	SD	*N*
112.9	9.1	4.7	147	14.2	4.2	54	24.3	6.1	89
115.0	9.6	3.9	120	16.1	3.8	34	23.1	3.5	80
116.9	9.9	3.2	111	15.9	3.9	39	235	7.9	76
118.9	9.3	2.8	106	15.5	4.1	33	21.7	5.0	79
121.3	7.8	2.2	101	13.1	35	47	19.2	3.9	83
124.5	5.9	2.0	80	11.3	3.0	36	18.2	5.0	65
127.8	4.4	1.7	80	9.8	2.8	42	16.7	5.8	82
1995									
91.1	18.2	7.8	104	26.9	8.9	71	35.8	5.9	50
93.6	15.8	8.1	88	25.8	7.1	50	33.1	4.8	44
97.0	12.5	6.0	126	20.3	7.0	61	28.0	4.8	54
99.1	11.2	5.7	156	19.2	6.1	80	27.1	5.3	75
100.5	11.7	5.5	103	20.0	5.8	51	25.3	4.8	44
101.4	11.3	5.9	98	20.4	4.9	33	25.3	5.0	38
102.5	11.3	5.2	91	20.1	4.2	33	24.1	4.8	32
103.5	10.7	4.8	90	18.8	5.2	38	24.4	4.7	34
104.4	12.0	4.4	82	18.2	3.4	41	23.6	3.8	36
107.5	9.0	3.2	81	14.4	2.8	50	22.5	6.2	34
109.6	9.5	3.6	99	15.5	6.1	49	20.8	4.4	45
112.0	8.5	3.4	108	13.7	5.0	65	19.4	4.8	53
114.1	7.0	3.3	99	11.2	3.0	63	18.2	4.0	51
116.0	7.0	3.8	129	11.7	4.4	90	17.2	4.1	64
118.1	5.5	3.3	128	9.7	4.3	104	16.4	4.6	66
120.0	5.0	2.8	126	9.6	4.0	112	14.7	3.0	71
122.0	5.3	2.6	80	8.4	2.8	61	14.3	3.5	44
123.0	5.2	1.7	114	8.9	2.8	99	14.1	2.5	75
125.0	4.8	2.6	151	8.4	3.1	122	13.6	2.9	100
129.1	5.2	3.2	123	10.9	4.5	89	16.4	6.3	54
131.0	5.5	3.2	117	11.5	4.5	108	15.8	4.5	42
1996									
101.1	9.3	5.9	98	13.0	4.4	131	18.8	3.9	66
107.5	7.9	4.9	102	12.9	5.6	96	19.3	5.2	39
109.9	7.8	3.8	128	13.2	6.4	93	18.3	6.3	61
114.9	8.3	5.5	90	14.7	6.7	68	18.8	5.9	41
Mean	9.1			14.7			20.8		
Minimum	4.0			8.1			12.5		
Maximum	18.2			26.9			35.8		

Note: Minimum, maximum, and mean values are give at the bottom of the table. Day 100 is April 10 in non-leap years.

1989–1995 data, so the predictions were independent of the 1996 data. The downstream passage distributions for the 1996 cohorts were combined to generate one distribution for all the cohorts at each of the observation sites. The predicted and observed cumulative passage distributions were then compared to assess the utility of the model as a predictive tool.

Results

The constant migration rate model (model 1) gave a mean migration rate of 11.78 km·day^{-1} through the entire system (Table 2). The plot of observed versus modeled mean travel time indicates that this model is inadequate for describing fish migration (Fig. 3). The model predicted roughly the same travel times to each observation site for all of the cohorts.

The linear flow component (model 2) explained 52.1% of the variability in the first model (Table 2). Although model 2 offers an improvement over model 1, some spread and bias is evident (Fig. 3). Under this model, the fish used 76% of the river for downstream migration.

Introducing a flow–season interaction (model 3) substantially improved model performance, increasing the R^2 to 0.804 (Table 2). With this model, the fish used less river flow before the seasonal inflection point (day 113 or April 23 in non-leap years) and substantially more later in the season. Model 3 underestimated shorter travel times and overestimated longer travel times (Fig. 3).

The experience factor added to the nonflow term (model 4) corrected the bias of model 3, increasing the R^2 to 0.895. The

Table 2. Parameter estimates, standard errors, sums of squares, and R^2 for the four migration rate models for all cohorts in the years 1989–1996.

Model	Parameter estimates (SE)							Residual SS	R^2
	β_{MIN}	β_{MAX}	α_1	β_{FLOW}	α_2	T_{SEASN}	σ^2		
1	11.78 (0.40)						366.83 (11.40)	7817.99	
2	–3.01 (0.24)			0.764 (0.018)			240.16 (6.71)	3743.90	0.521
3	2.77 (0.28)			0.794 (0.030)	0.138 (0.013)	113.26 (1.16)	139.30 (3.31)	1532.49	0.804
4	0.85 (0.07)	15.79 (4.06)	0.126 (0.053)	0.579 (0.012)	0.123 (0.008)	109.44 (0.78)	139.81 (3.03)	817.34	0.895
4[a]	0.97 (0.06)	17.21 (7.66)	0.109 (0.074)	0.539 (0.024)	0.153 (0.016)	107.87 (0.81)	134.45 (2.98)	723.14	

Note: The model 4 parameter estimates for the cohorts with the 1996 data omitted are also provided. The units for β_{MIN} and β_{MAX} are km·day^{-1}; α_1 and α_2 are in units·day^{-1}; β_{FLOW} is nondimensional; T_{SEASN} has units of day of the year; and σ^2 is expressed in km^2·day^{-1}. For models 1–3, β_{MIN} in this table corresponds to β_0.

[a]1996 omitted.

Fig. 3. Observed mean travel time versus modeled mean travel time for each of the four migration rate models for 1989–1996. The travel times are from Snake River Trap to each of the observations sites: Lower Granite, Little Goose, and McNary dams. Each point represents a cohort at a single observation site; therefore, each cohort is represented three times in each plot. **x**, mean travel time to Lower Granite Dam; ●, mean travel time to Little Goose Dam; **+**, mean travel time to McNary Dam.

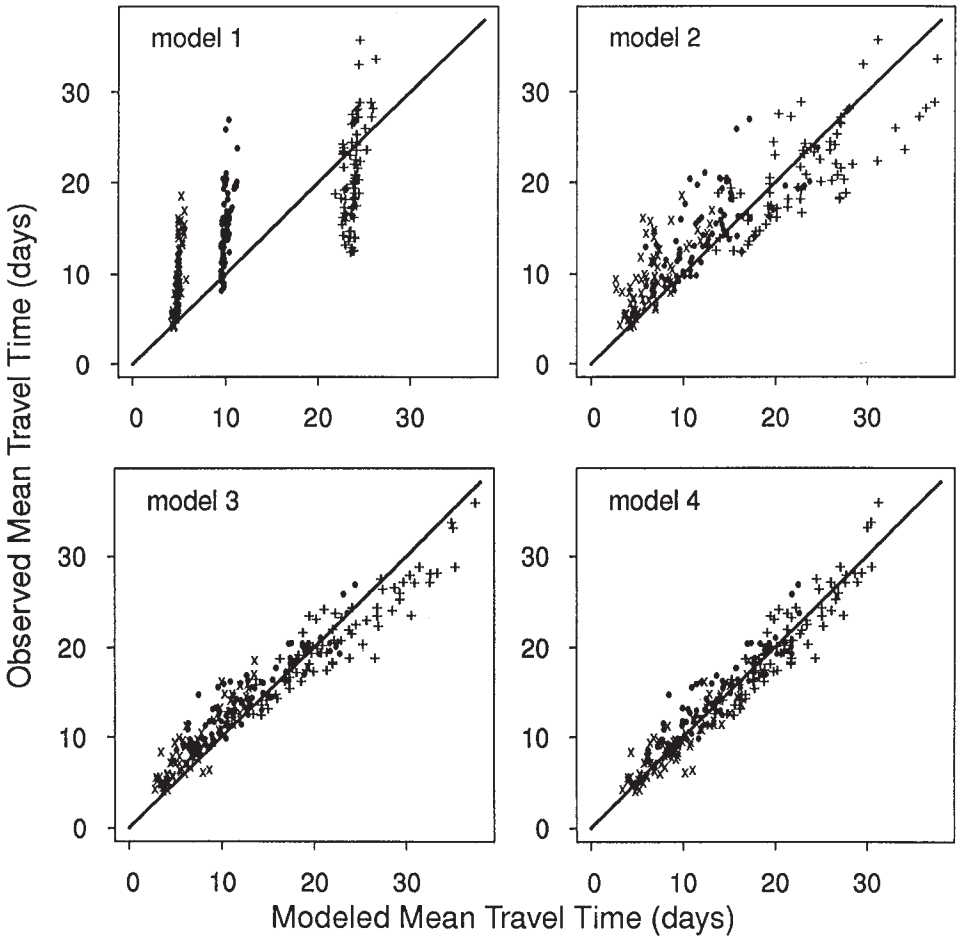

flow-independent maximum migration rate (β_{MAX}) was over 15 km·day^{-1} faster than the minimum rate (β_{MIN}). With a value of 0.126 for α_1, flow-independent migration rate attained over 95% of the difference between β_{MAX} and β_{MIN} within 30 days, which is less than the maximum observed travel time between Snake River Trap and McNary Dam. A value of 0.123 for α_2 indicated that fish required approximately 48 days to range from 5 to 95% of maximal flow usage. The standard errors were small compared with the parameter values, indicating that this model is stable.

As model performance improved, the estimated value for σ^2 decreased. Recall that σ^2 describes the rate of spreading of the cohort as it moves downstream. Some of the variability ascribed to population spreading in the less complex models was

actually due to lack of fit of the migration rate model. As the ability to predict migration rate improved, so did the precision of predicting the individual cohort's behavior.

Model 4 successfully predicted the arrival distribution at Lower Granite Dam with only slight deviations between expected and observed arrival distributions (Fig. 4). The predictions were accurate at Little Goose Dam for the first 50% of passage, but fish arrived later than expected during the last half of the season. At McNary Dam, the early fish migrated faster than predicted, and the later fish migrated slower than expected.

Discussion

Comparing travel time data with a sequence of nested models is a powerful way to determine the appropriate level of model complexity. In this analysis, the data supported the more complex models. The model with the seasonal flow term (model 3) improved model fit considerably compared with the model with the simpler linear flow term (model 2), indicating that the effect of flow on the Snake River yearling chinook has a seasonal component. Model 4 removed the bias present in model 3 by increasing the migration rate as the fish progressed downstream.

While the most complex model could describe a variety of behaviors and predict mean travel times to three observation points, it was still relatively simple in terms of number of parameters: six migration rate parameters and one spread parameter. This model explained 90% of the variability present in the constant migration rate model, even with the wide range of observed mean travel times (observed mean travel times for Snake River Trap to Lower Granite Dam ranged from 4.0 to 18.2 days, for Snake River Trap to Little Goose Dam ranged from 8.1 to 26.9 days, and for Snake River Trap to McNary Dam ranged from 12.5 to 35.8 days (Table 1)).

We selected these hierarchical models based on our ideas of mechanisms affecting smolt migration. Choosing models prior to conducting the statistical analysis is, in our opinion, more valid than multiple regressions that look at all possible factors and potentially suffer from unplanned tests (Sokal and Rohlf 1981). The procedure of examining data at several observation sites within a single analysis and using many release groups per year enables the detection of complex migratory behavior that is not detectable with standard regression analyses.

Although we applied the model to Snake River yearling chinook, we did not design the model specifically for these fish. The model is general and can be readily applied to other anadramous species. In the future, we plan to use the model to characterize the range of behaviors demonstrated by Columbia and Snake River salmonids.

Our results are consistent with other studies of juvenile salmonid travel time. Flow has been demonstrated as an important factor in determining travel times of yearling chinook and steelhead (*Oncorhynchus mykiss*) through the Columbia and Snake rivers (Berggren and Filardo 1993; Smith et al. 1993). Seasonal behavior was observed by Bax (1982), who determined that juvenile salmonids in the Hood Canal in Washington migrated close to the shore early in the season and further offshore later in the season, and by Johnson and Groot (1963), who determined that sockeye salmon (*Oncorhynchus nerka*)

Fig. 4. Comparisons of predicted and observed cumulative passage versus date at the three observation sites for the 1996 migration year. The solid line represents the data and the dotted line represents the model prediction. The prediction was based on parameters derived from 1989–1995 data. One set of parameters was used to generate predictions to all three sites. Day 100 is April 10 in non-leap years.

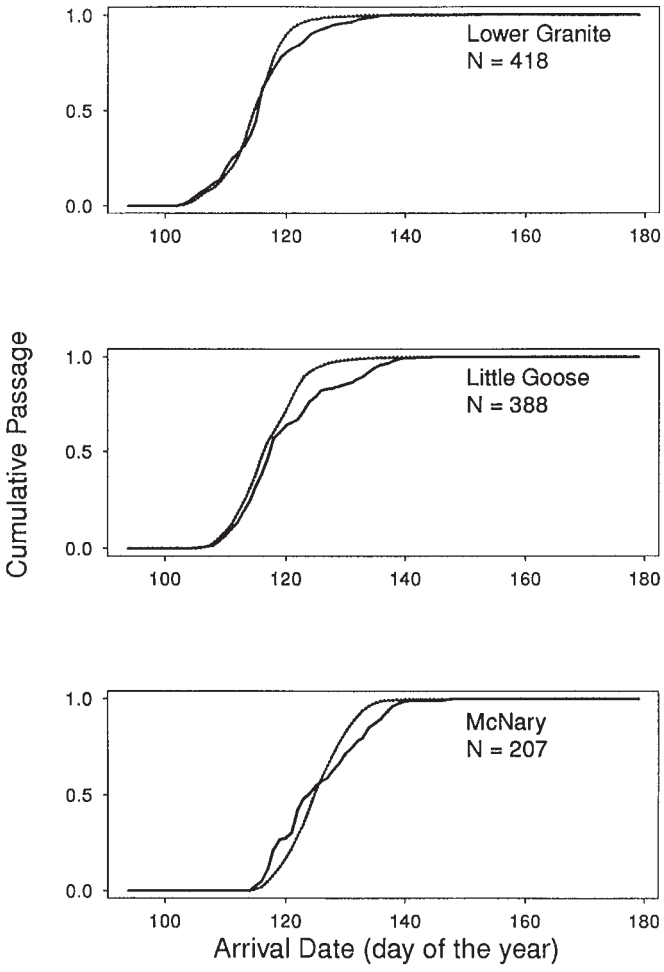

increased migration rate later in the season. The seasonal response may be a result of elevated levels of smoltification later in the season. Smoltification is the sequence of physiological changes preparing juvenile salmonids for the saltwater habitat (Folmar and Dickhoff 1980). Beeman and Rondorf (1994) demonstrated that higher levels of ATPase activity (a measure of smoltification) were associated with faster migration rates in spring chinook. In addition, several researchers have demonstrated the importance of photoperiod (Hoar 1976; Giorgi et al. 1990; Muir et al. 1994) to migration rate and timing; accelerated photoperiod resulted in faster migration rates.

Although our results provide additional evidence that juvenile salmon behavior is not constant during downstream migration, further research is needed to clearly identify the mechanisms that lead to the observed patterns. For instance, the magnitude of the flow effect is determined by current preferences and the proportion of the day spent migrating. These behaviors have not been extensively quantified on a seasonal basis for juvenile salmonids migrating through reservoirs.

Understanding the complexity of migratory behavior should improve hydro operations designed to decrease travel time. The linear flow model, which has been the basis of many mitigation proposals, assumes that increases in migration rate are directly proportional to increases in river velocity. Our seasonal flow model implies that fish response to increased river velocities will vary throughout the season. In addition, the downstream acceleration term indicates that fish in lower reaches migrate faster and might not need increased river velocities. With these factors in mind, flow augmentation and drawdown programs could be timed to maximize benefits to the fish while minimizing costs and detrimental effects.

The passage predictions for the 1996 fish (Fig. 4) further illustrate the capabilities of the model as a management tool. Arrival distributions are useful for in-season decisions such as the scheduling of spill, flow augmentation, and fish transportation. Deviations between predicted and observed patterns can also lead to further explorations of migratory behavior, and future refinements to the model will focus on improving its predictive capabilities.

Acknowledgments

We acknowledge the Bonneville Power Administration for funding this work, contract No. DE-BI79-89BP02347, project No. 89-108. We also thank Joshua Hayes, Chris Van Holmes, and two anonymous reviewers for comments and criticisms on various drafts of this paper.

References

Anderson, J.J., Hayes, J.A., Shaw, P.A., and Zabel, R.W. 1996. Columbia River Salmon Passage Model CRiSP 1.5: Theory, calibration, validation. Spec. Publ., Bonneville Power Administration, Portland, Oreg.

Bates, D.M., and Watts, D.G. 1988. Nonlinear regression analysis and its applications. John Wiley & Sons, New York.

Bax, N. J. 1982. Seasonal and annual variations in the movement of juvenile chum salmon through Hood Canal, Washington. *In* Salmon and trout migratory behavior symposium. *Edited by* E.L. Brannon and E.O. Salo. Contrib. 793, School of Fisheries, University of Washington, Seattle, Wash.

Beeman, J.B., and Rondorf, D.W. 1994. Estimating the effects of river flow, smoltification, and other biotic and abiotic variables on the travel time of juvenile salmonids in the Columbia and Snake rivers. *In* Assessment of smolt condition for travel time analysis. Prepared by A.G. Maule, J.B. Beeman, R.M. Schrock, and P.V. Harner. Report to the Bonneville Power Administration, Portland, Oreg. Project No. 87-401.

Berggren, T.J., and Filardo, M.J. 1993. An analysis of variables influencing the migration of juvenile salmonids in the Columbia River basin. N. Am. J. Fish. Manage. **13**: 48–63.

Brett, J.R., Hollands, M., and Alderdice, D.F. 1958. The effect of temperature on the cruising speed of young sockeye and coho salmon. J. Fish. Res. Board Can. **15**: 587–605.

Buettner, E.W., and Nelson, V.L. 1990. Smolt monitoring at the head of Lower Granite Reservoir and Lower Granite Dam. Report to the Bonneville Power Administration, Portland, Oreg. Project No. 83–323 B,

Draper, N.R., and Smith, H. 1981. Applied regression analysis. John Wiley & Sons, New York.

Fletcher, R. 1990. Practical methods of optimization. 2nd ed. John Wiley & Sons, New York.

Folmar, C.F., and Dickhoff, W.W. 1980. The parr–smolt transformation (smoltification) and seawater adaptation in salmonids. Aquaculture, **21**: 1–37.

Gill, P.E., Murray, W., and Wright, M. 1981. Practical optimization. Academic Press, London, U.K.

Giorgi, A.E., Swan, G.E., Zaugg, W.D., and McCutcheon, S. 1990. Biological manipulation of migration rate: the use of advanced photoperiod to accelerate smoltification in yearling chinook salmon. Annual Report of Research Financed by Bonneville Power Administration (Agreement DE-A179-88-BP50301) and Coastal Zone and Estuarine Studies Division. Northwest Alaska Fisheries Center, National Marine Fisheries Center, National Oceanic and Atmospheric Administration, Washington, D.C.

Groot, C., and Margolis, L. 1991. Pacific salmon life histories. University of British Columbia Press, Vancouver, B.C.

Hoar, W.S. 1976. Smolt transformation: evolution, behavior, and physiology. J. Fish. Res. Board Can. **33**: 1234–1252.

Iwamoto, R.N., Muir, W.D., Sandford, B.P., McIntyre, K.W., Frost, D.A., Williams, J.G., Smith, S.G., and Skalski, J.R. 1994. Survival estimates for the passage of juvenile chinook salmon through Snake River dams and reservoirs. Annual Report, 1993. U.S. Department of Energy, Bonneville Power Administration, Portland, Oreg. Contract No. DE-AI79-93BP10891.

Johnson, W.E., and Groot, C. 1963. Observations on the migration of young sockeye salmon (*Oncorhynchus nerka*) through a large, complex lake system. J. Fish. Res. Board Can. **20**: 919–937.

Muir, W.D., Zaugg, W.S., Giorgi, A.E., and McCutcheon, A.E. 1994. Accelerating smolt development and downstream movement in yearling chinook salmon with advanced photoperiod and increased temperature. Aquaculture, **123**: 387–399.

Muir, W.D., Smith, S.G., Iwamoto, R.N., Kamikawa, D.J., McIntyre, K.W., Hockersmith, E.E., Sandford, B.P., Ocker, P.A., Ruehle, T.E., Williams, J.G., and Skalski, J.R. 1995. Survival estimates for the passage of juvenile salmonids through Snake River dams and reservoirs. Annual Report, 1994. U.S. Department of Energy, Bonneville Power Administration, Portland, Oreg., contract No. DE-AI79-93BP10891, and U.S. Army Corps of Engineers, Walla Walla District, Walla Walla, Wash., contract No. E86940119.

Muir, W.D., Smith, S.G., Hockersmith, E.E., Achord, S., Absolon, R.F., Ocker, P.A., Eppard, B., Ruehle, T.E., Williams, J.G., Iwamoto, R.N., and Skalski, J.R. 1996. Survival estimates for the passage of yearling chinook salmon and steelhead through Snake River dams and reservoirs. Annual Report, 1995. U.S. Department of Energy, Bonneville Power Administration, Portland, Oreg., contract No. DE-AI79-93BP10891, and U.S. Army Corps of Engineers, Walla Walla District, Walla Walla, Wash., contract No. E86940119.

NMFS (National Marine Fisheries Service). 1995. Proposed recovery plan for Snake River salmon. National Marine Fisheries Service and the National Oceanic and Atmospheric Administration, Washington, D.C.

Prentice, E.F., Flagg, T.A., and McCutcheon, C.S. 1990. Feasibility of using implantable passive integrated transponder (PIT) tags in salmonids. Am. Fish. Soc. Symp. **7**: 317–322.

Press, W.H., Flannery, B.P., Teukolsky, S.A., and Vetterling, W.T. 1994. Numerical recipes in C. Cambridge University Press, Cambridge, U.K.

Raymond, H.L. 1979. Effects of dams and impoundments on migrations of juvenile chinook salmon and steelhead from the Snake River, 1966 to 1975. Trans. Am. Fish. Soc. **108**: 505–529.

Seber, G.A.F., and Wild, C.J. 1989. Nonlinear regression. John Wiley & Sons, New York.

Smith, S.G., Skalski, J.R., and Giorgi, A.E. 1993. Statistical evaluation of travel time estimation based on data from freeze-branded chinook salmon on the Snake River, 1982–1990. Prepared for U.S. Department of Energy, Bonneville Power Administration, Department of Fish and Wildlife, Portland, Oreg. Contract No. DE-B179-91BP35885.

Sokal, R.R., and Rohlf, F.J. 1981. Biometry. W.H. Freeman and Company, New York.

Washington, P.M. 1982. The influence of the size of juvenile coho salmon (*Oncorhynchus kisutch*) on seaward migration and survival. *In* Salmon and Trout Migratory Behavior Symposium. *Edited by* E.L. Brannon and E.O. Salo. Contrib. 793, School of Fisheries, University of Washington, Seattle, Wash.

Weisberg, S. 1980. Applied linear regression. John Wiley & Sons, New York.

Zabel, R.W. 1994. Spatial and temporal models of migrating juvenile salmon with applications. Ph.D. thesis, University of Washington, Seattle, Wash.

Zabel, R.W., and Anderson, J.J. 1997. A model of the travel time of migrating juvenile salmon, with an application to Snake River spring chinook. N. Am. J. Fish. Manage. **17**: 93–100.